Agricultural and Forest Meteorology 247 (2017) 365–375

Contents lists available at ScienceDirect

Agricultural and Forest Meteorology

journal homepage: www.elsevier.com/locate/agrformet

Research Paper

Retrieving vegetation canopy water content from hyperspectral thermal measurements

Elnaz Neinavaz*, Andrew K. Skidmore, Roshanak Darvishzadeh, Thomas A. Groen

Department of Natural Resources, Faculty of Geo-Information Science and Earth Observation (ITC), University of Twente, Hengelosestraat 99, 7500 AE, Enschede, The Netherlands

ARTICLE INFO

Keywords:
Fuel moisture content
Equivalent water thickness
Spectral emissivity
Thermal infrared
Canopy
Hyperspectral

ABSTRACT

The retrieval of vegetation canopy water content using thermal hyperspectral (TIR, 8–14 μm) measurements is investigated in this study. Vegetation water content indicators such as fuel moisture content (FMC, %, mass-based) and equivalent water thickness (EWT, g cm^{-2}, area based) play significant roles in plant physiology, as well as in the modelling of fire risk and behavior, particularly in forests. Although retrieval of these parameters, in particular EWT, has been demonstrated from optical and TIR measurements, to our knowledge their prediction at canopy level in the thermal part of the electromagnetic spectrum has not yet been investigated. Therefore, the application of hyperspectral TIR data for predicting FMC and EWT parameters at canopy level is explored here. The emissivity of spectral data in the TIR region is measured for four species (*Azalea japonica*, *Buxus sempervirens*, *Euonymus japonicus*, and *Ficus benjamina*) under controlled laboratory conditions, using a portable MIDAC Fourier transform infrared spectrometer. EWT, FMC, and their corresponding canopy emissivity measurements are assessed by destructive sampling of the leaves. Leaf area, as well as fresh and dry mass of the harvested leaves, is determined for all four species. Partial least square regression and artificial neural networks, using various spectral subsets, are used to predict the two variables of interest. Higher estimation accuracies have been obtained for both FMC and EWT at canopy level using artificial neural networks. Unexpectedly, the FMC at canopy level, as a mass-based variable, more accurately retrieved using either method. This is contrary to previous findings using multispectral and hyperspectral data. Our results suggest that plant mass may play a greater role in determining spectral emissivity than plant area does.

1. Introduction

In the past decades, remote sensing has been recognized as a tool to monitor and quantify vegetation variables. Canopy biophysical and biochemical variables involved in biophysical processes of terrestrial ecosystems (e.g. carbon and water cycling) determine how plants respond to environmental factors and influence ecosystem processes as well as responses to climate change. Vegetation water content is an indication of vegetation physiological condition and terrestrial ecosystem status (Claudio et al., 2006). It plays a significant role in the understanding of the earth's ecosystem functioning (Clevers and Kooistra, 2006) when assessing drought status in forestry and agriculture (Peñuelas and Filella, 1998), or estimating wildfire occurrence (Chuvieco et al., 2004). For instance, biochemical processes (e.g. photosynthesis and evaporation) are limited by vegetation water content (Peñuelas et al., 1994). Flammability in a forest, a critical parameter in fire ignition, also depends on vegetation water content (i.e., Fuel Moisture Content (FMC) in forest fire literature). The principal indicators used in remote sensing that characterize the amount of water in vegetation are fuel moisture content (FMC, %) and equivalent water thickness (EWT, g cm^{-2}) (Colombo et al., 2008). EWT is the amount of water per unit leaf area (Clevers et al., 2010; Hunt and Rock, 1989; Jacquemoud and Baret, 1990). In remote sensing studies EWT is at times also expressed as vegetation liquid water content (Cheng et al., 2006). FMC can be defined as the ratio between the water quantity in the fuel (the difference between fresh and dry weight) and either the fresh weight or the dry weight (Ceccato et al., 2001; Danson et al., 1992). FMC is highly correlated with risk of wildfire (Chuvieco et al., 2004; Hunt et al., 2013) and is described as leaf water content or leaf gravimetric water content in remote sensing studies (Buitrago et al., 2016; Ceccato et al., 2002a; Ceccato et al., 2001; Colombo et al., 2008; Ullah et al., 2014). In this study, EWT and FMC are considered to be indicators for area-based and mass-based vegetation water content, respectively. Area-based variables are valuable from a plant physiological point of view. Transpiration, respiration, gas exchange (e.g. uptake of CO_2 and H_2O), as well as plant physiochemical processes of

* Corresponding author.
E-mail addresses: e.neinavaz@utwente.nl (E. Neinavaz), a.k.skidmore@utwente.nl (A.K. Skidmore), r.darvish@utwente.nl (R. Darvishzadeh), t.a.groen@utwente.nl (T.A. Groen).

http://dx.doi.org/10.1016/j.agrformet.2017.08.020
Received 13 October 2016; Received in revised form 4 August 2017; Accepted 16 August 2017

photosynthesis (e.g. carbon fixation), occur as a flux per unit leaf surface area (Hikosaka, 2004; Lloyd et al., 2013). Mass-based parameters are important for estimating carbon flux, as well as growth in leaves.

In the past decades, retrieval of these variables from remote sensing data was investigated using a broad range of approaches (Gao, 1996; Gao and Goetzt, 1995; Serrano et al., 2000). The majority of these studies focused on the visible, near-infrared (VNIR, 0.3–1.0 μm), and shortwave-infrared (SWIR 1.0–2.5 μm) regions (Ali et al., 2015; Ceccato et al., 2002a; Clevers and Kooistra, 2006; Clevers et al., 2010; Dawson et al., 1999; Jin and Liu, 1997; Kalaitzidis et al., 2010; Laurin et al., 2014; Mirzaie et al., 2014; Qi et al., 2014; Tucker, 1980; Ustin et al., 1998; Yebra et al., 2013; Zhu et al., 2015), as well as on mid-wave infrared (2.5–6 μm) (Ullah et al., 2013). Estimation of EWT and FMC using remote sensing data has posed different challenges. Verbesselt et al. (2007) and Chuvieco et al. (2003) state that operational estimation of EWT is difficult in the field because it requires the calculation of leaf area; while Jacquemoud and Baret (1990) demonstrate that it is a challenge to predict FMC due to the difficulty in calculating vegetation dry matter content (DMC, g m^{-2}). Despite the fact that both EWT and FMC provide information on the amount of water present in vegetation, estimation of EWT using empirical and physical models has been more successful than FMC when using remote sensing data (Colombo et al., 2008). Moreover, it has been demonstrated that EWT relates better to spectral reflectance measurement (Ceccato et al., 2002b; Danson and Bowyer, 2004) and its estimation is less problematic than FMC's from remote sensing data in the VNIR and SWIR regions (Colombo et al., 2008; Danson and Bowyer, 2004). In contrast, it is hard to generalize the relationship between FMC and spectral reflectance as the found relationships in the optical domain (VNIR/SWIR) differ in previous studies (Chuvieco et al., 2003; Chuvieco et al., 2002; Paltridge and Barber, 1988; Pinol et al., 1998). In this respect, using thermal infrared hyperspectral data (TIR, 8–14 μm) opens new opportunities for estimating FMC for vegetation studies, particularly in forestry applications to model the fire risk.

To our knowledge, spectral emissivity from hyperspectral thermal data has been poorly studied in the past and has not yet been used to retrieve EWT and FMC from multiple plant species at canopy level. A few studies have attempted to relate emissivity spectra in the TIR domain to vegetation water content at leaf level using hyperspectral TIR data (Buitrago et al., 2016; Ullah et al., 2012). Recently, Ullah et al. (2014) revealed that the MIR domain is a highly sensitive spectral region for estimating water content at the leaf level, using narrow band indices developed from hyperspectral MIR and TIR data. Their findings show that the optimal narrow-band indices in the TIR region are the wavebands 11.31 μm and 11.46 μm.

Additionally, little is known about properties of vegetation in the TIR region, while the TIR offers a wide atmospheric window with large transparency which makes this region suitable for remote sensing studies (Clerbaux et al., 2011). Remote sensing data from the VNIR-SWIR alone is not sufficient to explain the structural and chemical characteristics of vegetation. For instance, the spectral features resulting from the combination of primary absorption features in the VNIR and SWIR regions, make it challenging to link particular wavebands to an individual chemical constituent, due to overlapping absorption features of plant biochemical contents (Kokaly et al., 2009). Moreover, the spectral profiles of plant species in the VNIR and SWIR regions are mostly similar in shape because reflectance spectra in these regions are conquered by absorption features of chemical components weighted by their concentrations and to a great extent, masked by water (Kokaly and Clark, 1999). In contrast, recent studies in the TIR domain demonstrated that leaf water content is the most important parameters associated with variations in TIR spectra (Buitrago et al., 2017), and also that the response of emissivity spectra (in particular for fresh leaves) are linked to structure and thickness of cuticle as well as leaf water content (Buitrago et al., 2016).

To scale EWT and FMC up from leaf level up to canopy level requires considering leaf area index (LAI, $m^2\ m^{-2}$) as an indispensable variable. This study considers both EWT and FMC variables at canopy level (hereafter referred to as EWT_C and FMC_C, respectively) and reflects on the applicability of emissivity spectra from hyperspectral TIR data to estimate the EWT_C and FMC_C, using partial least square regression (PLSR) and artificial neural networks (ANN). To estimate these variables from emissivity spectra in the TIR region, we conducted a laboratory experiment, measuring emissivity spectra for four plant species in the thermal infrared domain between 8 μm and 14 μm.

2. Materials and methods

2.1. Vegetation measurements

Four different plant species were selected: *Azalea japonica* (Azalea) (n = 10), *Buxus sempervirens* (Common box) (n = 10), *Euonymus japonicus* (Japanese spindle) (n = 11), and *Ficus benjamina* (Weeping fig) (n = 6). To create variation in the variables values of interest (i.e., EWC_C and FMC_C) and their corresponding canopy emissivity, leaves from different layers of the canopy were randomly removed in 3–4 consecutive steps (depending on the plant size) hence after each removal phase, the total value of the considered variables were lowered. The destructive sampling of the 37 plants thus yielded 144 estimates for both EWT_C and FMC_C. The leaf harvesting was executed within a couple of hours to minimize possible changes in the plant's physiological status, such as stomatal conductance, and to capture the potential interference of different physiological processes as a result of these defoliations. The leaf area of the harvested leaves was measured using a LI-3000C portable leaf area meter (LICOR, NE, USA).

2.2. Calculation of vegetation water indicators

The mass of the freshly harvested leaves from each sample was precisely weighed, using a digital weight balance with a 100 μg accuracy, immediately after harvesting. Leaves were then oven-dried at 75° C for 48 h until a constant weight was attained. EWT was computed using the following equation (Colombo et al., 2008):

$$EWT = \frac{W_f - W_d}{A \times P_w} \quad (1)$$

where w_f and w_d stand for a given sample's fresh and dry mass, respectively, A is sample leaf area and, P_w is a physical constant representing the density of pure water (1 g cm^{-3}).

LAI is the one-sided leaf area (m^2) per unit of horizontal surface area (m^2) (Watson, 1947). To calculate the LAI ($m^2\ m^{-2}$), the measured surface areas of the leaves (m^2) were divided by the corresponding ground area of the canopy (m^2). By multiplying EWT with the LAI, the total canopy water content per unit of ground area (EWT_C, g cm^{-2}) is obtained (Clevers et al., 2010; Yebra et al., 2013):

$$EWT_C = EWT \times LAI \quad (2)$$

EWT and FMC refer to two different quantities and describe vegetation water content in a different way (Ceccato et al., 2001; Ghulam et al., 2007). Several methods have been proposed to measure FMC. Since FMC is controlled and determined by EWT and dry matter content (DMC) according to $FMC = {}^{EWT}/_{DMC}$ (Jacquemoud and Baret, 1990), Riaño et al. (2005) predicted FMC by separately predicting EWT and DMC. They assumed vegetation DMC to be constant throughout the year. However, this assumption is not necessarily valid, particularly during drought periods. Garnier et al. (2001) observed that vegetation DMC decreased during a period of drought due to reduced productivity. In addition, these variables (i.e., EWT and DMC) are entirely independent of each other. Therefore, in this study, the most common Eq. (3) which is used by many researchers (Chuvieco et al., 1999; Desbois et al., 1997) is applied to calculate FMC. For scaling up of FMC, Hunt et al. (2012) estimated FMC_C by multiplying leaf EWT and DMC by LAI.

In this respect, FMC_C is estimated by multiplying FMC by LAI.

$$FMC = \frac{W_f - W_d}{W_f \ or \ W_d} \times 100 \quad (3)$$

$$FMCc = \frac{W_f - W_d}{W_f \ or \ W_d} \times LAI \quad (4)$$

2.3. Laboratory conditions

To create optimal measurement conditions and reduce any possible error from changing atmospheric conditions or temperature, measurements were carried out under controlled laboratory conditions, with walls, ceiling, and ground coated with a black material (Avis Aqua Blackboard Black) and plastic of known emissivity. The traditional procedure when measuring emissivity is to heat samples (e.g. geological samples) to a temperature above the ambient condition to create a thermal contrast (Ribeiro da Luz and Crowley, 2007; Salisbury, 1998). However, such treatment stresses plant samples, so instead we held the laboratory temperature at 10 °C, thus generating a suitable thermal contrast with the plants, which were kept at room temperature (20 °C) and only briefly (individually) transferred to the cool laboratory room to make the spectral measurements. Because Cheng et al. (2006) revealed that EWT_C is under-estimated in a semi-arid ecosystem due to a significant proportion of the soil background being mistakenly included as canopy closure, the background soil was covered with black plastic of known emissivity to minimize possible soil effects. We measured the emissivity spectra of the black plastic using a BRUKER Vertex 70 laboratory FTIR spectrometer. The black plastic had low emissivity and was assumed to cause minimal interference with the thermal radiance measurements of the samples.

2.4. Canopy spectroscopic measurement

2.4.1. Thermal infrared emission spectroscopy

The radiance spectra were measured using a portable FTIR spectrometer (Model M4401-F; MIDAC Corporation, CA, USA). The MIDAC configuration enables measurement of radiance spectra within the spectral range of 2.5 μm to 20 μm with an adjustable spectral resolution of 32–0.5 cm^{-1} (Eisele et al., 2015). The MIDAC has a liquid-nitrogen-cooled Mercury-Cadmium-Telluride (MCT) detector and customized foreoptics that consist of a flat folding mirror on a rotational axis, which allows measurements of two internal blackbodies (hot and cold) for calibration and measuring each sample. The MIDAC's folding mirror was kept at nadir position above the samples. The MIDAC's field of view (using a cut-off point of 5% of the maximum responsivity) has a starting diameter of 53 mm at the folding mirror and spreads with about 18 mrad. Since the amount of thermal emission varies according to the distance between the sample and the sensaor (Ribeiro da Luz and Crowley, 2007), and in order to reduce atmospheric attenuation (Korb et al., 1996), measurements were made with a fixed vertical distance between sensor and sample (60 cm).

The emissivity spectra of plant canopies were obtained using a series of FTIR measurements performed in the following order: radiance measurements of the hot blackbody, radiance measurement of the cold blackbody, radiance measurement of the sample (the plant canopy), and finally, radiance measurements of a highly diffuse reflecting gold plate (Infragold®). The temperature of the hot and cold blackbodies was checked between the measuring of each sample. The cold blackbody temperature was set just below the ambient temperature, at 5 °C (Korb et al., 1996). The hot blackbody temperature was set above the sample temperature, at 30 °C (Hori et al., 2006; Salvaggio and Miller, 2001). Details of the radiometric calibration of the blackbodies radiances can be found in Hook and Kahle (1996). A diffuse reflecting gold plate with an emissivity of ~0.04 was used to measure downwelling radiance (DWR) to correct radiance measurements and determine any significant influence of laboratory background emissions (Eisele et al., 2015). The infragold plate was placed directly under the MIDAC sensor at the same distance as the sample. The temperature of the sample, the infragold plate, and the laboratory was frequently monitored before and after each measurement, using thermistors (FLUKE 51 II Thermometer and Precision IR Thermometer) to detect any possible changes in temperature. Such changes in temperature could disturb the thermal contrast and result in over- or under-estimation of the emissivity values. The measurement series took less than five minutes each to minimize possible temperature drift of the instrument, physiological changes in the plants, and fluctuations in laboratory temperature (Hori et al., 2006).

The radiance spectra of the plant canopies were measured at wavelengths of 2.5 μm and 20 μm with a resolution of 2 cm^{-1}. On average, 32 scans were performed for each sample. The canopy emissivity measurements included 279 wavebands between 8 μm and 14 μm. Measurements outside this range had very low signal strength and were therefore excluded from further analysis. After each set of measurements, the canopy was rotated 90 ° clockwise, and the series of measurements was repeated until the canopy was fully rotated. The final corresponding canopy emissivity spectra of each sample for a particular value of FMC_C and EWT_C was then calculated from the average of four sets of measurements (covering 360°). The position of the MIDAC sensor above the canopy was kept constant. In total, 576 (4*144) canopy radiance measurements were obtained from the four plant species.

2.5. Data preprocessing

Spectral emissivity of the plants was calculated from their absolute radiance using the following equation (Korb et al., 1996),

$$\varepsilon_{sam}(\lambda) = \frac{L_{sam}(\lambda) - L_{DWR}(\lambda)}{B(\lambda, T_{sam}) - L_{DWR}(\lambda)} \quad (5)$$

where $\varepsilon_{sam}(\lambda)$ denotes the directional emissivity of the sample at wavelength λ, $L_{sam}(\lambda)$ is the spectral radiance from the target, T_{sam} is the actual physical temperature of the sample, $B(\lambda, T_{sam})$is the Planck function at wavelength λ and the sample temperature, and $L_{DWR}(\lambda)$ is the total spectral DWR from the hemisphere above the sample. To retrieve canopy surface emissivity, the information regarding the precise surface temperature (T_{sam}) at the time of the measurement is essential. Therefore, despite measuring canopy temperature before and after each measurement, the blackbody fit method was used to estimate the exact sample surface temperature value at the time of measurement. Details on the blackbody fit method can be found in Kahle and Alley (1992) and Salvaggio and Miller (2001). A Savitzky–Golay filter with a frame size of 15 data points and second- degree polynomial was used to reduce the noise in the canopy emissivity spectra (Savitzky and Golay, 1964). Data were analyzed and processed using MATLAB R2013b (Mathwork, Inc).

2.6. Estimation of variables

2.6.1. Partial least square regression

Hyperspectral data have a high dimensionality and also a high degree of collinearity in adjacent wavebands. This challenge is somewhat overcome using partial least squares regression (PLSR), one of the most used multivariate statistical techniques in hyperspectral studies, which transforms the variables into new orthogonal (Abdel-Rahman et al., 2014; Abdi, 2010; Chin et al., 2003). PLSR has been broadly applied as a multivariate quantitative technique in remote sensing vegetation analysis (Cho et al., 2007; Kooistra et al., 2004). It is a successful empirical approach to derive biochemical and biophysical properties from canopy spectral data in the VNIR (Asner and Martin, 2008; Darvishzadeh et al., 2008; Mirzaie et al., 2014), as well as biochemical and biophysical variables at both leaf and canopy level from emissivity spectra in the TIR region (Neinavaz et al., 2016b; Ullah et al., 2014). It

Table 1
The statistics of the variables measured per plant species. LAI represents the leaf area index; EWT_C is the canopy equivalent water thickness, EWT is the equivalent water thickness, FMCc is the canopy fuel moisture content, and FMC is the fuel moisture content.

Species	Variables	Min	Max	Mean Statistic	Mean Std. Error	Std. Deviation	Sample size
Buxus sempervirens	LAI ($m^2\ m^{-2}$)	1.17	9.80	4.548	0.344	2.149	30
	EWT_C ($g\ cm^{-2}$)	0.03	0.20	0.108	0.008	0.04	
	EWT ($g\ cm^{-2}$)	0.01	0.08	0.027	0.002	0.01	
	FMC_C	0.79	5.09	3.046	0.269	1.32	
	FMC (%)	46.54	84.58	69.215	1.773	8.68	
Azalea japonica	LAI ($m^2\ m^{-2}$)	0.60	3.35	1.573	0.099	0.543	30
	EWT_C ($g\ cm^{-2}$)	0.02	0.08	0.047	0.002	0.01	
	EWT ($g\ cm^{-2}$)	0.02	0.04	0.030	0.0008	0.004	
	FMC_C	0.51	2.60	1.254	0.076	0.42	
	FMC (%)	71.00	80.42	75.321	0.514	2.81	
Euonymus japonicus	LAI ($m^2\ m^{-2}$)	1.25	7.43	3.281	0.199	1.324	44
	EWT_C ($g\ cm^{-2}$)	0.08	0.16	0.113	0.004	0.02	
	EWT ($g\ cm^{-2}$)	0.03	0.05	0.038	0.001	0.004	
	FMC_C	1.43	3.68	2.379	0.156	0.68	
	FMC (%)	74.79	80.18	78.46	0.337	1.46	
Ficus benjamina	LAI ($m^2\ m^{-2}$)	1.04	8.36	3.601	0.329	1.805	30
	EWT_C ($g\ cm^{-2}$)	0.03	0.19	0.105	0.008	0.04	
	EWT ($g\ cm^{-2}$)	0.2	0.5	0.030	0.001	0.009	
	FMC_C	0.99	6.99	3.118	0.278	1.52	
	FMC (%)	79.88	95.00	87.040	0.736	4.03	

is a “full spectrum” method, which has the advantage that it makes use of all available spectral wavelengths (Haaland and Thomas, 1988). Here, PLSR analysis was used to determine the relative contribution of the 279 wavebands of the canopy emissivity spectra (independent variables) to explain variation in EWT_C and FMC_C for all the sampled species. The canopy emissivity spectra as independent variables were mean-centered before performing the PLSR analysis. An optimal number of factors was determined to avoid overfitting and to prevent collinearity, using cross-validation procedures with the root mean squared error ($RMSE_{cv}$) as a quality indicator. An optimal number of factors indicates the number of the extracted factor for which the total prediction error is minimized. A cross-validation procedure, also known as the “leave one out method” (Duda and Hart, 1973), is a method for selecting a model according to its predictive ability (Shao, 1993). In cross validation each data point is successively “left out” from the data and used as the validation set. The criterion for adding an extra factor to the model was that it would decrease the $RMSE_{CV}$ by > 2% (Geladi and Kowalski (1986)). Details on the basic PLSR algorithm can be found in Geladi and Kowalski (1986) and Williams and Norris (1987). All PLSR analyses were carried out using the TOMCAT toolbox 1.01 within MATLAB (Daszykowski et al., 2007). Since β coefficients represent the contribution of each waveband to the model, they were utilized to determine the importance of wavebands in each fitted PLSR model. The thresholds for β coefficients were specified according to their standard deviations. Wavebands with a β coefficient above this threshold were considered to be contributing significantly. The sign of the β coefficients (i.e. plus or minus) represents the direction of the relationship between emissivity value (i.e., independent variable) and FMC_C and EWT_C (i.e., dependent variable). The higher absolute value of β coefficients represents the stronger relation.

2.6.2. Artificial neural networks

The use of artificial neural networks (ANN) has been shown to be an effective alternative to more traditional statistical techniques (Paliwal and Kumar, 2009). Recently, Neinavaz et al. (2016b) demonstrated the significance of using ANN for the prediction of LAI using hyperspectral TIR data. The multi-layer perceptron is a broadly utilized neural network in remote sensing studies (Atzberger, 2004; Mirzaie et al., 2014). A typical ANN consists of different types of layers, namely: input layers, hidden layers, and output layers. Three different data sets were employed as input layer, comprising (1) all available canopy emissivity values in 279 wavebands between 8 μm and 14 μm (labelled as ANW); (2) the most important wavebands which were identified from PLSR analysis (labelled as IPW); (3) the best performing narrow bands as determined by Ullah et al. (2014) (labelled as UIPW). For network training, two algorithms were considered: the Levenberg-Marquardt (LMANN) and the Scaled Conjugate Gradient (ScgANN) algorithm, and they were applied as two common training algorithms in back-propagation networks to develop models for the estimation of our variables of interest. Although there are no rules that determine the optimal number of hidden layers, an increase in the number of hidden layers enable the network to tackle more complex problems (Atkinson and Tatnall, 1997). For instance, Skidmore et al. (1997) revealed that higher accuracy is obtained with three hidden layers, than with two or one. As the prediction performance of ANN depends on the number of neurons in the hidden layer, the best ANN size was identified by testing different numbers. The early stopping technique was utilized to avoid overfitting problems. In this technique, training stops as soon as performance on a validation data set begins to worsen (Nowlan and Hinton, 1992). Furthermore, linear regression analyses were performed between the predicted and the measured values of EWT_C and FMC_C to determine the best ANN model. The cross-validation procedure was repeated 1000 times, and results were averaged to reduce unfavorable effects from the random initialization of the optimization routine. The reliability of ANNs in estimating our variables was evaluated using the cross-validated coefficient of determination (R^2_{CV}) and the cross-validated root mean squared error ($RMSE_{CV}$). All analyses were carried out using the MATLAB neural network toolbox.

3. Results

3.1. Relationship between canopy variables and emissivity spectra

The measured EWT_C and FMC_C values demonstrated a wide range [0.02–0.2 for EWT_C; and 0.51–6.99 for FMC_C] due to the variation in the leaf shapes and sizes of the plants. The summary of the statistics concerning these variables is presented for each species in Table 1. As can be observed from this Table 1, *Azalea japonica* has the lowest value for EWT_C and FMC_C, while *Ficus benjamina* and *Buxus sempervirens* have the highest values for FMC_C and EWT_C, respectively.

The relationship between EWT and LAI, as well as FMC and LAI, were studied when the data were pooled using the coefficient of

Table 2
The performance of partial least square regression for estimating canopy equivalent thickness (EWT_C, g cm^{-2}), and canopy fuel moisture content (FMC_C). $RMSE_{CV}$ is the relative cross-validated root mean squared error and R^2 is the coefficient of determination.

Species	Variable	No. of Factors	R^2	$RMSE_{CV}$	SD of β Coeff	Important wavebands (μm)
Ficus benjamina	EWT_C	3	0.672	0.024	0.094	8.8, 10.6, 10.7, 10.8, 13.2–13.5
	FMC_C	4	0.757	0.875	3.766	8.8, 11.9, 12.0, 13.7–14
Azalea japonica	EWT_C	5	0.810	0.003	0.035	8.0, 8.1, 8.2, 8.8, 10.4
	FMC_C	5	0.807	0.180	3.360	8.3–8.6, 8.8, 9.5
Euonymus japonicus	EWT_C	4	0.789	0.012	0.138	8.3, 8.8, 9.6, 9.8, 9.9, 10.4, 10.5
	FMC_C	3	0.804	0.442	4.410	8.1, 8.3, 8.8, 9.6, 9.9, 10.0, 10.3–10.5
Buxus sempervirens	EWT_C	4	0.589	0.025	0.088	8.0, 8.5, 8.8, 9.2–9.5, 11.1, 13.5, 13.8–14.0
	FMC_C	5	0.730	0.704	7.031	8.0, 8.8, 9.0, 9.1, 9.3, 11.1, 12.0–12.3, 12.5, 13.0, 13.5
Pooled data	EWT_C	5	0.390	0.030	0.111	8.8, 9.0, 9.4, 9.6, 10.1, 11.4, 11.8, 11.9, 12.3, 14.0
	FMC_C	5	0.429	1.076	3.776	8.7, 8.8, 9.4–9.7, 10.1, 11.1, 11.7–11.9, 13.7

determination (R^2). The results reveal that LAI has a negative relationship with EWT (R^2 = 0.25) and FMC (R^2 = 0.05). In addition, the result showed that a poor relation exists between EWT and FMC (R^2 = 0.20) which confirms these variables effectively reflecting different properties.

3.2. Partial least square regression and vegetation water content variables

The most important wavebands for each species identified in the PLSR model are tabulated in Table 2. The number of factors included in each PLSR model range from three to five per species. The β coefficients associated with the PLSR model for estimation of EWT_C and FMC_C across the species and pooled data are shown in Fig. 2. As can be seen in Table 2, among the investigated species EWT_C and FMC_C have been accurately retrieved for *Azalea japonica* and least accurately retrieved for *Buxus sempervirens* addition, the results show that FMC_C is predicted more accurately than EWT_C. As can be seen from Fig. 2, standard deviations thresholds values are vary among the plant species. Additionally, among the most important wavebands (Table 2 and Fig. 2), waveband 8.8 μm is common to all the plant species, which could be related to the emission of oleanolic acid (Ribeiro da Luz and Crowley, 2007) or leaf compounds other than cellulose (Fabre et al., 2011).

3.3. Estimating vegetation water content using artificial neural networks

A comparative analysis of ANNs, resulting from the LMANN and ScgANN training algorithms with different network inputs, is tabulated in Table 3 and presents the estimated accuracy of the optimal ANN structure for each species. The reliability of ANNs for estimating EWT_C, and FMC_C is confirmed by the high values of R^2_{CV} and low values of $RMSE_{CV}$. The most remarkable result is that FMC_C is retrieved with higher accuracy than EWT_C for all four species. As can be seen in Table 3, in general, FMC_C and EWT_C are more accurately estimated with the LMANN than with the ScgANN training algorithm. This can be seen clearly in the estimation of both variables for *Ficus benjamina*, *Azalea japonica*, as well as the pooled data. However, for *Euonymus japonicus* the variables are more accurately estimated using the ScgANN algorithm; this is also the case for the EWT_C in *Buxus sempervirens* with all 279 narrow wavebands as network input.

Of the four species, *Euonymus japonicus* displays the most accurate estimation of FMC_C (R^2_{CV} = 0.89 and $RMSE_{CV}$ = 0.007) and EWT_C (R^2_{CV} = 0.91 and $RMSE_{CV}$ = 0.18). As can be seen in Table 3, wavebands important for estimating water content at leaf level (Ullah et al., 2014) used in ANN, result in the lowest accuracy for both FMC_C and EWT_C. The highest predicted accuracy using ANN is obtained using two and seven neurons, respectively, in hidden layers for EWT_C and FMC_C. The relationship between estimated and measured EWT_C, and FMC_C using ANN models is shown in Fig. 3. Additionally, the results in Table 3 demonstrate that using the most important wavebands, identified with PLSR as the network input, leads to higher prediction accuracy, than using all the 279 available wavebands does among four plant species. However, as can be seen from Table 3, using all 279 wavebands as network input achieved a higher prediction accuracy for the pooled data for both EWT_C and FMC_C variables.

4. Discussion

This study attempts to highlight how emissivity spectra from the TIR region can estimate mass based canopy water content (FMC_C) and area based canopy water content (EWT_C) with statistical methods (i.e., PLSR) and machine learning algorithms (i.e., ANN). Previous literature shows that EWT_C as an area-based variable can be estimated from water absorption features in the VNIR and SWIR spectral domains (Bowyer and Danson, 2004; Mirzaie et al., 2014). However, estimating the relationship between FMC_C and spectral data in the optical region remains problematic (Chuvieco et al., 2003; Paltridge and Barber, 1988). It seems that spectral information from these VNIR and SWIR is not adequate for retrieving FMC_C due to the internal structure of leaves as well as the influence of vegetation DMC (Bowyer and Danson, 2004; Ceccato et al., 2001). Our results demonstrate that both variables can be predicted reasonably well from TIR emissivity spectra. However, we demonstrate that mass-based canopy water content can be more accurately retrieved across species from hyperspectral TIR data (Tables 2 and 3) than area-based canopy water content. A possible justification for FMC_C being predicted more accurately than EWT_C using emissivity spectra may be the relation between FMC_C and the combination of heat flow and mass. FMC_C as a mass-based variable indirectly represents temperature and light use efficiency and also represents the water availability in the plant (Yebra et al., 2013).

In this study, FMC_C and EWT_C are calculated respectively by multiplying FMC and EWT with the LAI, which can be a proxy of mass. Recently Neinavaz et al. (2016a) found that there is a positive correlation between LAI and TIR emissivity spectra. As can be observed in Fig. 1, the correlation between LAI and EWT is higher (R^2 = 0.25) than between LAI and FMC (R^2 = 0.05). Therefore, when using LAI, one may expect to retrieve EWT_C with higher accuracy than FMC_C. However, this is not observed here. As FMC does not scale with LAI, which means that canopies with similar FMC may have varying LAI values (Fig. 1) and, consequently, differing spectral responses (Bowyer and Danson, 2004; Yebra et al., 2013). In addition, our results show that both FMC_C and EWT_C can be predicted with higher accuracy than LAI using TIR hyperspectral data (Neinavaz et al., 2016b).

Although in our study LAI was poorly correlated with EWT (leaf level), this relationship might not always be strictly valid under all conditions and may have different temporal (daily or seasonal) trends or vary across ecoregions (Trombetti et al., 2008). It should be noted that besides LAI some other factors such as canopy structure, temperature, species physiology as well as the environmental conditions

Table 3
Cross-validated results (R^2_{CV} and $RMSE_{CV}$) of estimated canopy equivalent water thickness (EWT_C) and canopy fuel moisture content (FMC_C), obtained using artificial neural networks with different network inputs structures, i.e., ANW is using All narrow wavebands, IPW is using Important wavebands identified by PLSR, and UIPW is using Optimal Waveband Index identified by (Ullah et al. 2014) as network input parameters. LMANN and ScgANN are Levenberg-Marquardt and Scaled Conjugate Gradient training algorithms, respectively.

Species	Input	Training algorithm	FMC_C			EWT_C		
			No. of neuron	R^2_{CV}	$RMSE_{CV}$	No. of neuron	R^2_{CV}	$RMSE_{CV}$ (g cm^{-2})
Ficus benjamina	ANW	LMANN	6	0.76	0.77	1	0.67	0.02
	IPW		6	0.90	0.49	5	0.88	0.01
	UIPW		7	0.21	1.38	2	0.49	0.03
	ANW	ScgANN	5	0.71	0.88	3	0.53	0.03
	IPW		6	0.80	0.71	4	0.78	0.02
	UIPW		5	0.20	1.39	4	0.26	0.04
Azalea japonica	ANW	LMANN	1	0.78	0.23	3	0.75	0.00
	IPW		1	0.91	0.13	2	0.57	0.01
	UIPW		3	0.57	0.28	7	0.46	0.012
	ANW	ScgANN	6	0.75	0.23	7	0.47	0.01
	IPW		7	0.85	0.17	4	0.48	0.01
	UIPW		6	0.26	0.37	6	0.39	0.011
Euonymus japonicus	ANW	LMANN	6	0.68	0.39	6	0.52	0.01
	IPW		7	0.91	0.18	2	0.89	0.007
	UIPW		6	0.21	0.67	6	0.30	0.02
	ANW	ScgANN	4	0.83	0.31	3	0.82	0.00
	IPW		6	0.81	0.34	2	0.74	0.01
	UIPW		6	0.17	0.63	6	0.19	0.02
Buxus sempervirens	ANW	LMANN	5	0.86	0.51	5	0.62	0.02
	IPW		3	0.91	0.40	5	0.70	0.02
	UIPW		7	0.28	1.57	3	0.41	0.03
	ANW	ScgANN	6	0.65	0.84	4	0.65	0.02
	IPW		6	0.79	0.61	5	0.69	0.02
	UIPW		6	0.19	1.23	6	0.16	0.03
pooled data	ANW	LMANN	5	0.74	0.76	5	0.51	0.03
	IPW		5	0.57	0.90	7	0.50	0.03
	UIPW		7	0.24	1.17	5	0.19	0.03
	ANW	ScgANN	5	0.50	0.95	5	0.49	0.03
	IPW		5	0.39	1.06	4	0.38	0.03
	UIPW		6	0.15	1.25	5	0.13	0.04

can have an influence on the amount of water content in vegetation (Aassine and El Jai, 2002; Atzberger et al., 2013; Serrano et al., 2000; Trombetti et al., 2008). In this study, due to the stable conditions provided during the laboratory measurements, potential variation caused by environmental conditions (e.g. temperature) may be ignored. However, further experimental work is required to confirm this assertion.

As can be seen in Tables 2 and 3, our results indicate that EWT_C (ANN: R^2_{CV} = 0.51, $RMSE_{CV}$ = 0.03) and FMC_C (ANN: R^2_{CV} = 0.74, $RMSE_{CV}$ = 0.76) have been predicted with moderate accuracy from the pooled data. However, these variables have been retrieved with higher accuracy at the species level. In other words, the observed relationships with TIR emissivity spectra using both proposed statistical techniques are likely to be species-specific. In this respect, the correlation between emissivity spectra in the TIR region and variation in cuticle composition in different plant species is a possible explanation (Elvidge, 1988; Salisbury, 1986). Recently, Buitrago et al. (2016) studied the correlation between leaf water content and TIR emissivity spectra and suggested that the plant's cuticle thickness and structure may be linked to the changes in emissivity spectra. Additionally the multi-functional properties of the cuticle, due to its heterogeneous structure and chemical nature (Khayet and Fernández, 2012), may additionally vary between e.g., species, genotypes, plant physiological status as well as environmental conditions during growth (Fernández et al., 2016, 2014; Guzmán-Delgado et al., 2016; Knoche et al., 2004; Szakiel et al., 2012), and could consequently affect the emissivity spectra. Moreover, the prediction of canopy water content (in terms of EWT_C and FMC_C) in the TIR domain could be affected by differences in the vegetation canopy architecture (Pinter et al., 1985) as well as canopy gap size (Ribeiro da Luz and Crowley, 2010) through the control of energy transfer (Kimes, 1980). Therefore, in order to obtain an accurate estimation of canopy parameters such as EWT_C and FMC_C in heterogeneous ecosystems, knowledge of other biophysical and biochemical properties of plant species is probably a prerequisite.

Our findings revealed that compared with PLSR models, the ANN approach obtained relatively higher prediction accuracy. This may be due to the fact that ANN method as a machine learning algorithm offers a powerful means of analyzing complex datasets without making assumptions about the model parameterization. Our results are in agreement with the previous finding of Neinavaz et al. (2016b) who revealed that ANN improves the prediction accuracy of canopy biophysical variables compared with PLSR using emissivity spectra over the entire TIR spectrum. Both methods (i.e., PLSR and ANN) have their strengths and limitations which have been addressed by many researchers (Cramer, 1993; Mehrotra et al., 1997; Pirouz, 2006).

Of the three categories of network input for ANN used to retrieve EWT_C and FMC_C, the important wavebands identified using PLSR (i.e., IPW) were superior to the others for the prediction of these variables for individual species (R^2_{CV} = 0.92, $RMSE_{CV}$ = 0.19 for FMC_C; and R^2_{CV} = 0.89, $RMSE_{CV}$ = 0.007 for EWT_C). In contrast, the ANW network input achieved a higher prediction accuracy (R^2_{CV} = 0.74, $RMSE_{CV}$ = 0.76 for FMC_C; and R^2_{CV} = 0.51, $RMSE_{CV}$ = 0.03 for EWT_C) for pooled data. A possible explanation is that by incorporating important wavebands into the back-propagation neural network as input variables, over-fitting was prevented and data dimension was reduced for individual plant species. It should be noted that previous studies have shown that emissivity spectra are species-specific over TIR region (Neinavaz et al., 2016b; Ribeiro da Luz and Crowley, 2007) and the spectral features in the TIR domain varied from one species to another (Fabre et al., 2011). Therefore, the ANW input network, which contains

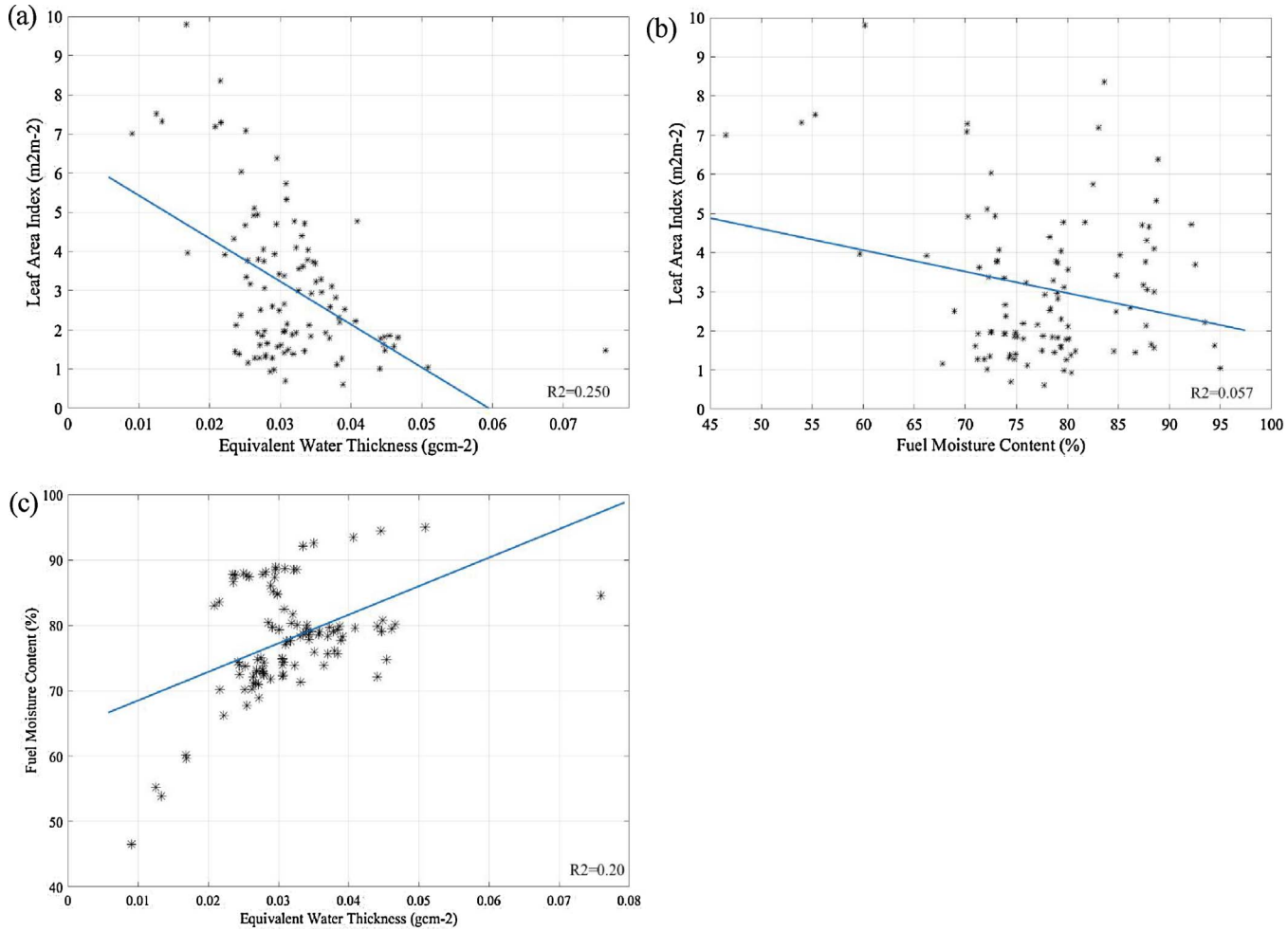

Fig. 1. Measured leaf area index ($m^2\ m^{-2}$) versus equivalent water thickness (g cm^2) (a), and estimated fuel moisture content (%) (b), and measured equivalent water thickness versus estimated fuel moisture content (c) for the pooled dataset.

279 wavebands, seems more suitable to use for pooled data. Wavebands identified by Ullah et al. (2014) achieved lower accuracies estimating both variables than other network inputs (Table 3). The reason for this may be that their study was carried out at leaf level and that the canopy structure and architecture of different plant species did not play any role in their findings.

In this study, we did not assess the strength of the entire spectra (i.e., VNIR-TIR region) for the retrieval of vegetation water content (i.e., FMC and EWT) at canopy level. However, since FMC_C was predicted with higher accuracy than EWT_C, which is contrary to previous findings using hyperspectral and multispectral data, further experimental efforts would be required to assess the improvement in prediction accuracy of FMC and EWT at canopy level over different regions of electromagnetic spectrum.

The results that are reported in this study are derived from emissivity measurements under controlled laboratory conditions. Accordingly, atmospheric absorption and scattering effects have been dismissed from our data set, and possible sources of error such as atmospheric corrections, and the effect of the background have been reduced. It will require further study to quantify the possible effect of these factors on the success of estimating EWC and FMC at canopy level from TIR spectra. However, this study provides an initial basis for evaluating the potential of thermal hyperspectral remote sensing for EWT_C and FMC_C prediction.

5. Conclusion

Our results demonstreted the value of thermal emissivity spectra from the TIR region for predicting FMC_C and EWT_C using multivariate statistical technique and machine learning algorithm (i.e., PLSR and ANN, respectively) at canopy level for multiple plant species. FMC_C as a representative of mass-based variables has been retrieved more accurately than EWT_C from hyperspectral TIR data. When pooled data of several plant species is considered, the prediction accuracy drops for both variables (i.e., EWT_C hand FMC_C). When combined with ANN, optimized narrow wavebands as network input data present the most satisfactory performance predicting EWT_C and FMC_C. Clearly, given the results of our experiments, it will be difficult, although not impossible, to extend our findings to airborne and satellite level, particularly in different ecosystems. Field conditions, including canopy structure and atmospheric conditions, coupled with the spatial and spectral resolution of satellite observations, may provide challenges when upscaling to canopy level. However, in our perspective, the findings of this study prove the concept of predicting vegetation water content at canopy level by means of hyperspectral TIR data to be valid.

Acknowledgments

This research received financial support from the EU Erasmus Mundus External Cooperation Window (EM8) Action 2, and was co-funded by the Natural Resources Department, Faculty of Geo-Information Science and Earth Observation (ITC), University of Twente,

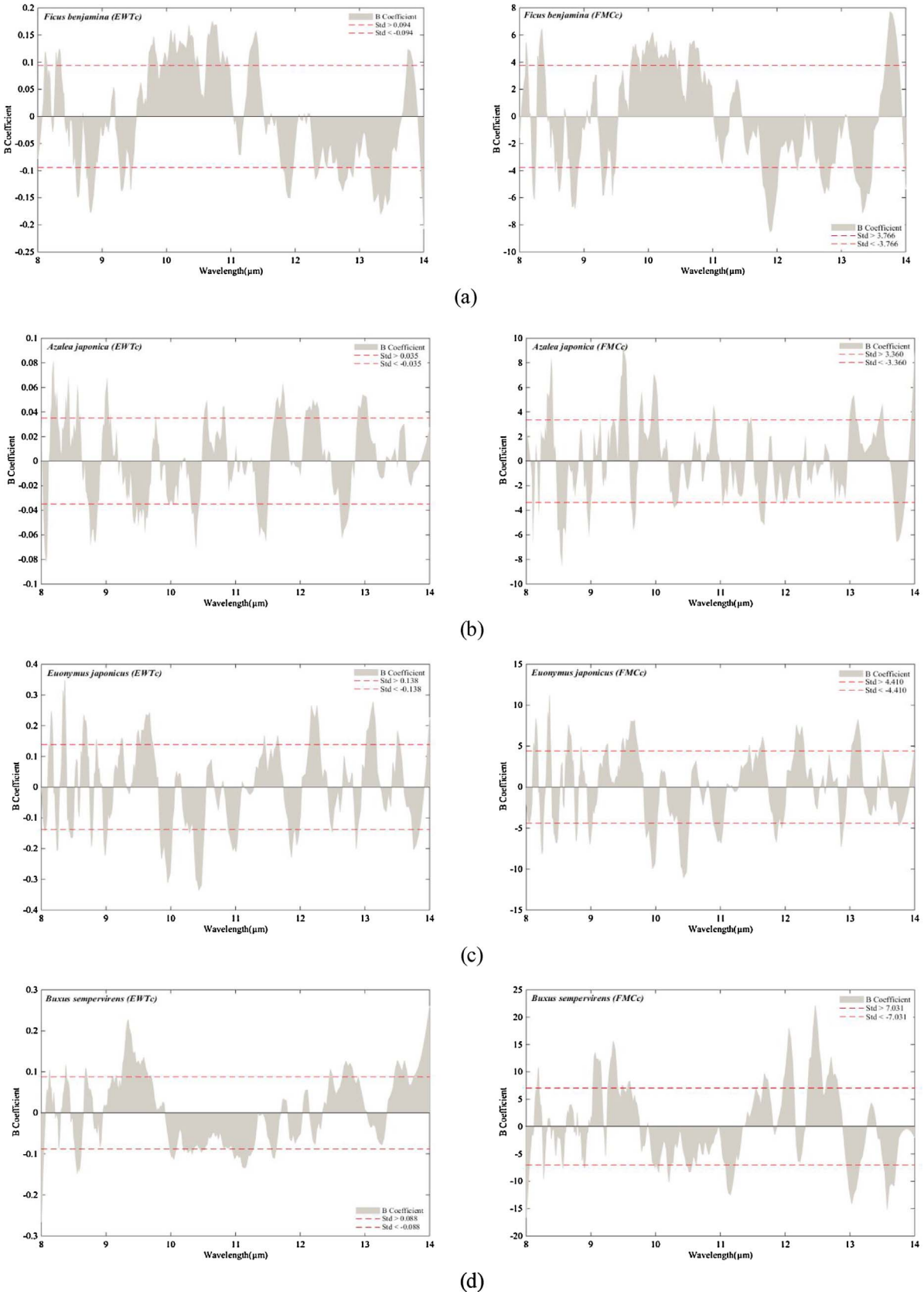

Fig. 2. The β coefficients associated with the PLSR model for canopy equivalent water thickness (EWT_C) (left side diagrams), and canopy fuel moisture content (FMC_C) (right diagrams) for the four species *Ficus benjamina* (a), *Azalea japonica* (b), *Euonymus japonicus* (c), and *Buxus sempervirens* (d). The threshold is based on the corresponding standard deviation of the β coefficient.

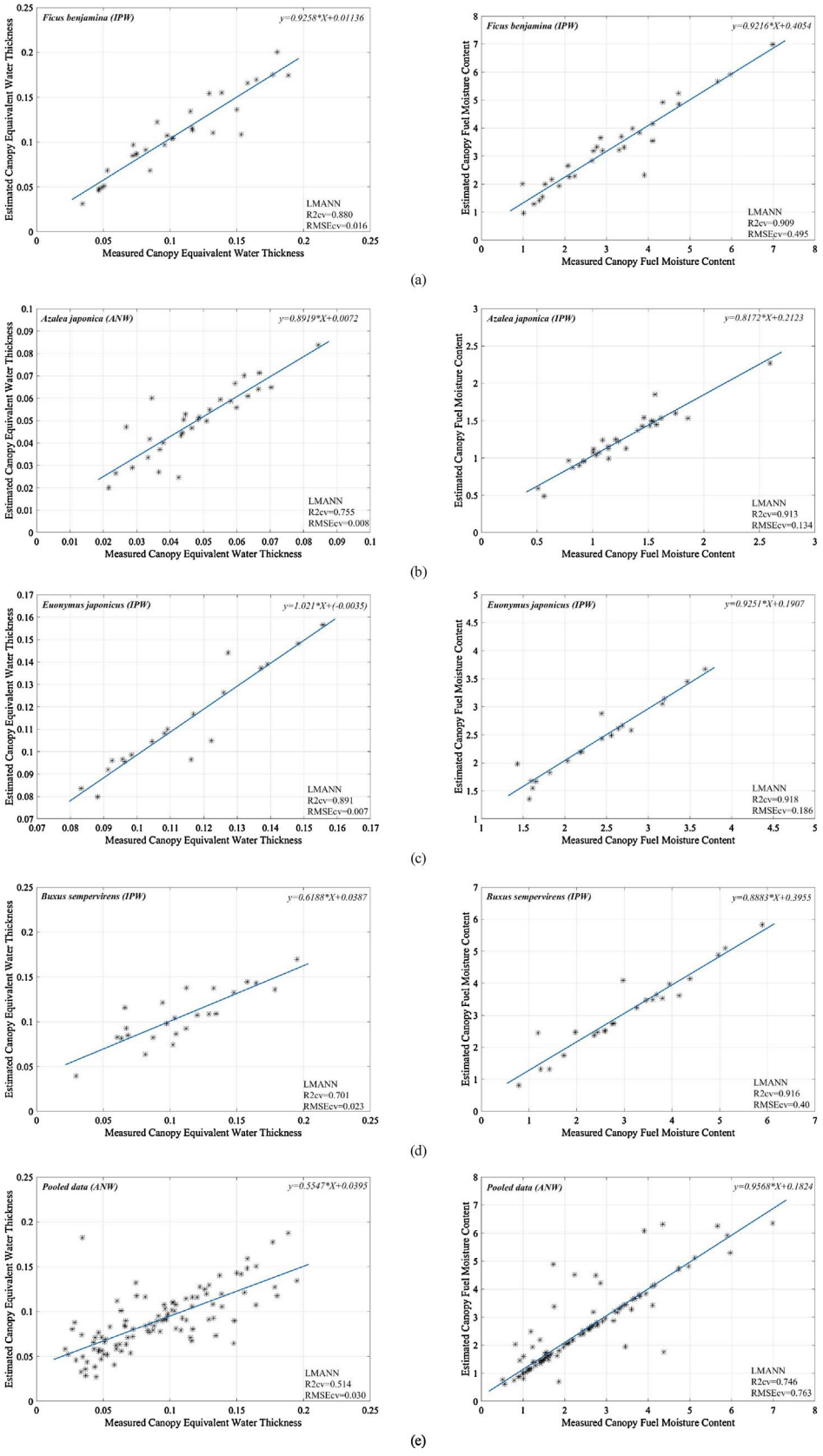

Fig. 3. Scatterplots of measured versus estimated canopy equivalent water thickness (EWT_C) (left side diagrams), and canopy fuel moisture content (FMC_C) (right side diagrams) for the four species *Ficus benjamina* (a), *Azalea japonica* (b), *Euonymus japonicus* (c), *Buxus sempervirens* (d), and Pooled data (e). The blue line represents a first order (linear) regression. (For interpretation of the references to colour in this figure legend, the reader is referred to the web version of this article.)

the Netherlands. The authors extend their appreciation for the great support received during laboratory measurements by Boudewijn de Smeth, Christoph Hecker and Watse Siderius of the Geoscience Laboratory at the ITC Faculty, University of Twente. We would like to thank Eva Skidmore for her editorial and linguistic advice on a near-final draft and Michal Daszykowski for helpful advice about TOMCAT toolbox. We thank the anonymous reviewers for their valuable comments.

References

Aassine, S., El Jai, M.C., 2002. Vegetation dynamics modelling: a method for coupling local and space dynamics. Ecol. Modell. 154, 237–249.

Abdel-Rahman, E.M., Mutanga, O., Odindi, J., Adam, E., Odindo, A., Ismail, R., 2014. A comparison of partial least squares (PLS) and sparse PLS regressions for predicting yield of Swiss chard grown under different irrigation water sources using hyperspectral data. Comput. Electron. Agric. 106, 11–19.

Abdi, H., 2010. Partial least squares regression and projection on latent structure regression (PLS Regression). Wiley Interdiscip. Rev. Comput. Stat. 2, 97–106.

Ali, I., Greifeneder, F., Stamenkovic, J., Neumann, M., Notarnicola, C., 2015. Review of machine learning approaches for biomass and soil moisture retrievals from remote sensing data. Remote Sensing 7, 16398–16421.

Asner, G.P., Martin, R.E., 2008. Spectral and chemical analysis of tropical forests: scaling from leaf to canopy levels. Remote Sens. Environ. 112, 3958–3970.

Atkinson, P.M., Tatnall, A., 1997. Introduction neural networks in remote sensing. Int. J. Remote Sens. 18, 699–709.

Atzberger, C., Darvishzadeh, R., Schlerf, M., Le Maire, G., 2013. Suitability and adaptation of PROSAIL radiative transfer model for hyperspectral grassland studies. Remote Sens. Lett. 4, 55–64.

Atzberger, C., 2004. Object-based retrieval of biophysical canopy variables using artificial neural nets and radiative transfer models. Remote Sens. Environ. 93, 53–67.

Bowyer, P., Danson, F., 2004. Sensitivity of spectral reflectance to variation in live fuel moisture content at leaf and canopy level. Remote Sens. Environ. 92, 297–308.

Buitrago, M.F., Groen, T.A., Hecker, C.A., Skidmore, A.K., 2016. Changes in thermal infrared spectra of plants caused by temperature and water stress. ISPRS J. Photogramm. Remote Sens. 111, 22–31.

Ceccato, P., Flasse, S., Tarantola, S., Jacquemoud, S., Grégoire, J.-M., 2001. Detecting vegetation leaf water content using reflectance in the optical domain. Remote Sens. Eviron. 77, 22–33.

Ceccato, P., Flasse, S., Grégoire, J.-M., 2002a. Designing a spectral index to estimate vegetation water content from remote sensing data: part 2. Validation and applications. Remote Sens. Environ. 82, 198–207.

Ceccato, P., Gobron, N., Flasse, S., Pinty, B., Tarantola, S., 2002b. Designing a spectral index to estimate vegetation water content from remote sensing data: part 1: theoretical approach. Remote Sens. Environ. 82, 188–197.

Cheng, Y.-B., Zarco-Tejada, P.J., Riaño, D., Rueda, C.A., Ustin, S.L., 2006. Estimating vegetation water content with hyperspectral data for different canopy scenarios: relationships between AVIRIS and MODIS indexes. Remote Sens. Environ. 105, 354–366.

Chin, W.W., Marcolin, B.L., Newsted, P.R., 2003. A partial least squares latent variable modeling approach for measuring interaction effects: results from a Monte Carlo simulation study and an electronic-mail emotion/adoption study. Inf. Syst. Res. 14, 189–217.

Cho, M.A., Skidmore, A., Corsi, F., Van Wieren, S.E., Sobhan, I., 2007. Estimation of green grass/herb biomass from airborne hyperspectral imagery using spectral indices and partial least squares regression. Int. J. Appl. Earth Obs. Geoinf. 9, 414–424.

Chuvieco, E., Deshayes, M., Stach, N., Cocero, D., Riaño, D., 1999. Short-term fire risk: foliage moisture content estimation from satellite data. Remote Sensing of Large Wildfires. Springer, pp. 17–38.

Chuvieco, E., Riano, D., Aguado, I., Cocero, D., 2002. Estimation of fuel moisture content from multitemporal analysis of Landsat Thematic Mapper reflectance data: applications in fire danger assessment. Int. J. Remote Sens. 23, 2145–2162.

Chuvieco, E., Aguado, I., Cocero, D., Riano, D., 2003. Design of an empirical index to estimate fuel moisture content from NOAA-AVHRR images in forest fire danger studies. Int. J. Remote Sens. 24, 1621–1637.

Chuvieco, E., Cocero, D., Riano, D., Martin, P., Martınez-Vega, J., de la Riva, J., Perez, F., 2004. Combining NDVI and surface temperature for the estimation of live fuel moisture content in forest fire danger rating. Remote Sens. Environ. 92, 322–331.

Claudio, H.C., Cheng, Y., Fuentes, D.A., Gamon, J.A., Luo, H., Oechel, W., Qiu, H.-L., Rahman, A.F., Sims, D.A., 2006. Monitoring drought effects on vegetation water content and fluxes in chaparral with the 970 nm water band index. Remote Sens. Environ. 103, 304–311.

Clerbaux, C., Drummond, J.R., Flaud, J.-M., Orphal, J., 2011. Using thermal infrared absorption and emission to determine trace gases. The Remote Sensing of Tropospheric Composition from Space. Springer, pp. 123–151.

Clevers, J., Kooistra, L., 2006. Using spectral information at the NIR water absorption features to estimate canopy water content and biomass. In: ISPRS Mid-Term Symposium Remote Sensing: From Pixels to Processes. Enschede, The Netherlands. pp. 8–11.

Clevers, J.G., Kooistra, L., Schaepman, M.E., 2010. Estimating canopy water content using hyperspectral remote sensing data. Int. J. Appl. Earth Obs. Geoinf. 12, 119–125.

Colombo, R., Meroni, M., Marchesi, A., Busetto, L., Rossini, M., Giardino, C., Panigada, C., 2008. Estimation of leaf and canopy water content in poplar plantations by means of hyperspectral indices and inverse modeling. Remote Sens. Environ. 112, 1820–1834.

Cramer, R.D., 1993. Partial least squares (PLS): its strengths and limitations. Perspect. Drug Dis. Des. 1 (2), 269–278.

Danson, F., Bowyer, P., 2004. Estimating live fuel moisture content from remotely sensed reflectance. Remote Sens. Environ. 92, 309–321.

Danson, F., Steven, M., Malthus, T., Clark, J., 1992. High-spectral resolution data for determining leaf water content. Int. J. Remote Sens. 13, 461–470.

Darvishzadeh, R., Skidmore, A., Schlerf, M., Atzberger, C., Corsi, F., Cho, M., 2008. LAI and chlorophyll estimation for a heterogeneous grassland using hyperspectral measurements. ISPRS J. Photogramm. Remote Sens. 63, 409–426.

Daszykowski, M., Serneels, S., Kaczmarek, K., Van Espen, P., Croux, C., Walczak, B., 2007. TOMCAT: a MATLAB toolbox for multivariate calibration techniques. Chemom. Intell. Lab. Syst. 85, 269–277.

Dawson, T., Curran, P., North, P., Plummer, S., 1999. The propagation of foliar biochemical absorption features in forest canopy reflectance: a theoretical analysis. Remote Sens. Environ. 67, 147–159.

Desbois, N., Deshayes, M., Beudoin, A., 1997. Protocol for fuel moisture content measurements. A Review of Remote Sensing Methods for the Study of Large Wildland Fires. pp. 61–72.

Duda, R.O., Hart, P.E., 1973. Pattern Classification and Scene Analysis. Wiley, New York.

Eisele, A., Chabrillat, S., Hecker, C., Hewson, R., Lau, I.C., Rogass, C., Segl, K., Cudahy, T.J., Udelhoven, T., Hostert, P., 2015. Advantages using the thermal infrared (TIR) to detect and quantify semi-arid soil properties. Remote Sens. Environ. 163, 296–311.

Elvidge, C.D., 1988. Thermal infrared reflectance of dry plant materials: 2.5–20.0 μm. Remote Sens. Environ. 26, 265–285.

Fabre, S., Lesaignoux, A., Olioso, A., Briottet, X., 2011. Influence of water content on spectral reflectance of leaves in the 3–15-domain. Geosci. Remote Sens. Lett. IEEE 8, 143–147.

Fernández, V., Guzmán, P., Peirce, C.A., McBeath, T.M., Khayet, M., McLaughlin, M.J., 2014. Effect of wheat phosphorus status on leaf surface properties and permeability to foliar-applied phosphorus. Plant Soil 384, 7–20.

Fernández, V., Guzmán-Delgado, P., Graça, J., Santos, S., Gil, L., 2016. Cuticle structure in relation to chemical composition: re-assessing the prevailing model. Front. Plant Sci. 7.

Gao, B.-C., Goetzt, A.F., 1995. Retrieval of equivalent water thickness and information related to biochemical components of vegetation canopies from AVIRIS data. Remote Sens. Environ. 52, 155–162.

Gao, B.-C., 1996. NDWI—a normalized difference water index for remote sensing of vegetation liquid water from space. Remote Sens. Environ. 58, 257–266.

Garnier, E., Laurent, G., Bellmann, A., Debain, S., Berthelier, P., Ducout, B., Roumet, C., Navas, M.L., 2001. Consistency of species ranking based on functional leaf traits. New Phytol. 152, 69–83.

Geladi, P., Kowalski, B.R., 1986. Partial least-squares regression: a tutorial. Anal. Chim. Acta 185, 1–17.

Ghulam, A., Li, Z.-L., Qin, Q., Tong, Q., Wang, J., Kasimu, A., Zhu, L., 2007. A method for canopy water content estimation for highly vegetated surfaces-shortwave infrared perpendicular water stress index. Sci. China Ser. D: Earth Sci. 50, 1359–1368.

Guzmán-Delgado, P., Graça, J., Cabral, V., Gil, L., Fernández, V., 2016. The presence of cutan limits the interpretation of cuticular chemistry and structure: Ficus elastica leaf as an example. Physiol. Plant. 157, 205–220.

Haaland, D.M., Thomas, E.V., 1988. Partial least-squares methods for spectral analyses: 1. Relation to other quantitative calibration methods and the extraction of qualitative information. Anal. Chem. 60, 1193–1202.

Hikosaka, K., 2004. Interspecific difference in the photosynthesis-nitrogen relationship: patterns, physiological causes, and ecological importance. J. Plant Res. 117, 481–494.

Hook, S.J., Kahle, A.B., 1996. The micro Fourier transform interferometer (μFTIR)—a new field spectrometer for acquisition of infrared data of natural surfaces. Remote Sens. Environ. 56, 172–181.

Hori, M., Aoki, T., Tanikawa, T., Motoyoshi, H., Hachikubo, A., Sugiura, K., Yasunari, T.J., Eide, H., Storvold, R., Nakajima, Y., 2006. In-situ measured spectral directional emissivity of snow and ice in the 8–14 μm atmospheric window. Remote Sens. Environ. 100, 486–502.

Hunt, E.R., Rock, B.N., 1989. Detection of changes in leaf water content using near-and middle-infrared reflectances. Remote Sens. Environ. 30, 43–54.

Hunt, E.R., Wang, L., Qu, J.J., Hao, X., 2012. Remote sensing of fuel moisture content from canopy water indices and normalized dry matter index. J. Appl. Remote Sens. 6, 061705.

Hunt Jr., E.R., Ustin, S.L., Riaño, D., 2013. Remote sensing of leaf, canopy, and vegetation water contents for satellite environmental data records. Satellite-Based Publications on Climate Change. Springer, pp. 335–357.

Jacquemoud, S., Baret, F., 1990. PROSPECT: a model of leaf optical properties spectra. Remote Sens. Environ. 34, 75–91.

Jin, Y.-Q., Liu, C., 1997. Biomass retrieval from high-dimensional active/passive remote sensing data by using artificial neural networks. Int. J. Remote Sens. 18, 971–979.

Kahle, A.B., Alley, R.E., 1992. Separation of temperature and emittance in remotely sensed radiance measurements. Remote Sens. Environ. 42, 107–111.

Kalaitzidis, C., Heinzel, V., Zianis, D., 2010. A review of multispectral vegetation indices for biomass estimation. In: Imagin [e, g] Europe: Proceedings of the 29th Symposium of the European Association of Remote Sensing Laboratories. IOS Press, Chania, Greece. p. 201.

Khayet, M., Fernández, V., 2012. Estimation of the solubility parameters of model plant surfaces and agrochemicals: a valuable tool for understanding plant surface interactions. Theor. Biol. Med. Model. 9, 1.

Kimes, D., 1980. Effects of vegetation canopy structure on remotely sensed canopy temperatures. Remote Sens. Environ. 10, 165–174.

Knoche, M., Beyer, M., Peschel, S., Oparlakov, B., Bukovac, M.J., 2004. Changes in strain and deposition of cuticle in developing sweet cherry fruit. Physiol. Plant. 120, 667–677.

Kokaly, R.F., Clark, R.N., 1999. Spectroscopic determination of leaf biochemistry using band-depth analysis of absorption features and stepwise multiple linear regression. Remote Sens. Environ. 67, 267–287.

Kokaly, R.F., Asner, G.P., Ollinger, S.V., Martin, M.E., Wessman, C.A., 2009. Characterizing canopy biochemistry from imaging spectroscopy and its application to ecosystem studies. Remote Sens. Environ. 113, S78–S91.

Kooistra, L., Salas, E., Clevers, J., Wehrens, R., Leuven, R., Nienhuis, P., Buydens, L., 2004. Exploring field vegetation reflectance as an indicator of soil contamination in

river floodplains. Environ. Pollut. 127, 281–290.
Korb, A.R., Dybwad, P., Wadsworth, W., Salisbury, J.W., 1996. Portable Fourier transform infrared spectroradiometer for field measurements of radiance and emissivity. Appl. Opt. 35, 1679–1692.
Laurin, G.V., Chen, Q., Lindsell, J.A., Coomes, D.A., Del Frate, F., Guerriero, L., Pirotti, F., Valentini, R., 2014. Above ground biomass estimation in an African tropical forest with lidar and hyperspectral data. ISPRS J. Photogramm. Remote Sens. 89, 49–58.
Lloyd, J., Bloomfield, K., Domingues, T.F., Farquhar, G.D., 2013. Photosynthetically relevant foliar traits correlating better on a mass vs an area basis: of ecophysiological relevance or just a case of mathematical imperatives and statistical quicksand? New Phytol. 199, 311–321.
Mehrotra, K., Mohan, C.K., Ranka, S., 1997. Elements of Artificial Neural Networks. MIT press.
Mirzaie, M., Darvishzadeh, R., Shakiba, A., Matkan, A., Atzberger, C., Skidmore, A., 2014. Comparative analysis of different uni-and multi-variate methods for estimation of vegetation water content using hyper-spectral measurements. Int. J. Appl. Earth Obs. Geoinf. 26, 1–11.
Neinavaz, E., Darvishzadeh, R., Skidmore, A.K., Groen, T.A., 2016a. Measuring the response of canopy emissivity spectra to leaf area index variation using thermal hyperspectral data. Int. J. Appl. Earth Obs. Geoinf. 53, 40–47.
Neinavaz, E., Skidmore, A.K., Darvishzadeh, R., Groen, T.A., 2016b. Retrieval of leaf area index in different plant species using thermal hyperspectral data. ISPRS J. Photogramm. Remote Sens. 119, 390–401.
Nowlan, S.J., Hinton, G.E., 1992. Simplifying neural networks by soft weight-sharing. Neural Comput. 4, 473–493.
Paliwal, M., Kumar, U.A., 2009. Neural networks and statistical techniques: a review of applications. Expert Syst. Appl. 36, 2–17.
Paltridge, G., Barber, J., 1988. Monitoring grassland dryness and fire potential in Australia with NOAA/AVHRR data. Remote Sens. Environ. 25, 381–394.
Peñuelas, J., Filella, I., 1998. Visible and near-infrared reflectance techniques for diagnosing plant physiological status. Trends Plant Sci. 3, 151–156.
Peñuelas, J., Gamon, J., Fredeen, A., Merino, J., Field, C., 1994. Reflectance indices associated with physiological changes in nitrogen-and water-limited sunflower leaves. Remote Sens. Environ. 48, 135–146.
Pinol, J., Filella, I., Ogaya, R., Peñuelas, J., 1998. Ground-based spectroradiometric estimation of live fine fuel moisture of Mediterranean plants. Agric. For. Meteorol. 90, 173–186.
Pinter Jr., P.J., Jackson, R.D., Elaine Ezra, C., Gausman, H.W., 1985. Sun-angle and canopy-architecture effects on the spectral reflectance of six wheat cultivars. Int. J. Remote Sens. 6, 1813–1825.
Pirouz, D.M., 2006. An overview of partial least squares.
Qi, Y., Dennison, P.E., Jolly, W.M., Kropp, R.C., Brewer, S.C., 2014. Spectroscopic analysis of seasonal changes in live fuel moisture content and leaf dry mass. Remote Sens. Environ. 150, 198–206.
Riaño, D., Vaughan, P., Chuvieco, E., Zarco-Tejada, P.J., Ustin, S.L., 2005. Estimation of fuel moisture content by inversion of radiative transfer models to simulate equivalent water thickness and dry matter content: analysis at leaf and canopy level. Geosci. Remote Sens. IEEE Trans. 43, 819–826.
Ribeiro da Luz, B., Crowley, J.K., 2007. Spectral reflectance and emissivity features of broad leaf plants: prospects for remote sensing in the thermal infrared (8.0–14.0 μm). Remote Sens. Environ. 109, 393–405.
Ribeiro da Luz, B., Crowley, J.K., 2010. Identification of plant species by using high spatial and spectral resolution thermal infrared (8.0–13.5 μm) imagery. Remote Sens. Environ. 114, 404–413.
Salisbury, J.W., 1986. Preliminary measurements of leaf spectral reflectance in the 8–14 μm region. Int. J. Remote Sens. 7, 1879–1886.
Salisbury, J., 1998. Spectral Measurements Field Guide. Published by the Defense Technology Information Center as Report No. ADA362372. Earth Satellite Corporation.
Salvaggio, C., Miller, C.J., 2001. Methodologies and protocols for the collection of mid-wave and longwave infrared emissivity spectra using a portable field spectrometer. Aerospace/Defense Sensing, Simulation, and Controls. International Society for Optics and Photonics, pp. 539–548.
Savitzky, A., Golay, M.J., 1964. Smoothing and differentiation of data by simplified least squares procedures. Anal. Chem. 36, 1627–1639.
Serrano, L., Ustin, S.L., Roberts, D.A., Gamon, J.A., Penuelas, J., 2000. Deriving water content of chaparral vegetation from AVIRIS data. Remote Sens. Environ. 74, 570–581.
Shao, J., 1993. Linear model selection by cross-validation. J. Am. Stat. Assoc. 88, 486–494.
Skidmore, A., Turner, B., Brinkhof, W., Knowles, E., 1997. Performance of a neural network: mapping forests using GIS and remotely sensed data. Photogramm. Eng. Remote Sens. 63, 501–514.
Szakiel, A., Pączkowski, C., Pensec, F., Bertsch, C., 2012. Fruit cuticular waxes as a source of biologically active triterpenoids. Phytochem. Rev. 11, 263–284.
Trombetti, M., Riaño, D., Rubio, M., Cheng, Y., Ustin, S., 2008. Multi-temporal vegetation canopy water content retrieval and interpretation using artificial neural networks for the continental USA. Remote Sens. Environ. 112, 203–215.
Tucker, C.J., 1980. Remote sensing of leaf water content in the near infrared. Remote Sens. Environ. 10, 23–32.
Ullah, S., Skidmore, A.K., Naeem, M., Schlerf, M., 2012. An accurate retrieval of leaf water content from mid to thermal infrared spectra using continuous wavelet analysis. Sci. Total Environ. 437, 145–152.
Ullah, S., Skidmore, A.K., Groen, T.A., Schlerf, M., 2013. Evaluation of three proposed indices for the retrieval of leaf water content from the mid-wave infrared (2–6 μm) spectra. Agric. For. Meteorol. 171, 65–71.
Ullah, S., Skidmore, A.K., Ramoelo, A., Groen, T.A., Naeem, M., Ali, A., 2014. Retrieval of leaf water content spanning the visible to thermal infrared spectra. ISPRS J. Photogramm. Remote Sens. 93, 56–64.
Ustin, S.L., Roberts, D.A., Pinzon, J., Jacquemoud, S., Gardner, M., Scheer, G., Castaneda, C.M., Palacios-Orueta, A., 1998. Estimating canopy water content of chaparral shrubs using optical methods. Remote Sens. Environ. 65, 280–291.
Verbesselt, J., Somers, B., Lhermitte, S., Jonckheere, I., Van Aardt, J., Coppin, P., 2007. Monitoring herbaceous fuel moisture content with SPOT VEGETATION time-series for fire risk prediction in savanna ecosystems. Remote Sens. Environ. 108, 357–368.
Watson, D.J., 1947. Comparative physiological studies on the growth of field crops: I. Variation in net assimilation rate and leaf area between species and varieties, and within and between years. Ann. Bot. 41–76.
Williams, P., Norris, K., 1987. Near-Infrared Technology in the Agricultural and Food Industries. American Association of Cereal Chemists, Inc.
Yebra, M., Dennison, P.E., Chuvieco, E., Riaño, D., Zylstra, P., Hunt, E.R., Danson, F.M., Qi, Y., Jurdao, S., 2013. A global review of remote sensing of live fuel moisture content for fire danger assessment: moving towards operational products. Remote Sens. Environ. 136, 455–468.
Zhu, X., Wang, T., Darvishzadeh, R., Skidmore, A.K., Niemann, K.O., 2015. 3D leaf water content mapping using terrestrial laser scanner backscatter intensity with radiometric correction. ISPRS J. Photogramm. Remote Sens. 110, 14–23.